

Interaction of PACAP with Sonic hedgehog reveals complex regulation of the Hedgehog pathway by PKA[☆]



Pawel Niewiadomski, Annie Zhujiang, Mary Youssef, James A. Waschek^{*}

Intellectual Development and Disabilities Research Center, The David Geffen School of Medicine, University of California, Los Angeles, Los Angeles, CA 90095, United States

ARTICLE INFO

Article history:

Received 23 May 2013

Received in revised form 17 June 2013

Accepted 12 July 2013

Available online 18 July 2013

Keywords:

Protein kinase A

Sonic hedgehog

PACAP

G-protein coupled receptors

Primary cilia

ABSTRACT

Sonic hedgehog (Shh) signaling is essential for proliferation of cerebellar granule cell progenitors (cGCPs) and its aberrant activation causes a cerebellar cancer medulloblastoma. Pituitary adenylate cyclase activating polypeptide (PACAP) inhibits Shh-driven proliferation of cGCPs and acts as tumor suppressor in murine medulloblastoma. We show that PACAP blocks canonical Shh signaling by a mechanism that involves activation of protein kinase A (PKA) and inhibition of the translocation of the Shh-dependent transcription factor Gli2 into the primary cilium. PKA is shown to play an essential role in inhibiting gene transcription in the absence of Shh, but global PKA activity levels are found to be a poor predictor of the degree of Shh pathway activation. We propose that the core Shh pathway regulates a small compartmentalized pool of PKA in the vicinity of primary cilia. GPCRs that affect global PKA activity levels, such as the PACAP receptor, cooperate with the canonical Shh signal to regulate Gli protein phosphorylation by PKA. This interaction serves to fine-tune the transcriptional and physiological function of the Shh pathway.

© 2013 The Authors. Published by Elsevier Inc. All rights reserved.

1. Introduction

The Sonic hedgehog (Shh) signaling pathway, which is involved in embryonic and postnatal development in humans and many other species, is also abnormally activated in several types of cancer [1]. The output of the pathway in vertebrates is mediated by a family of Gli transcription factors, but the processes that lead to Gli activation following the binding of Shh to its receptor Patched (Ptch) have not been fully elucidated [2]. It is known that Shh causes activation of a 7-transmembrane domain (7-TM) protein Smoothened (Smo), which under basal conditions is suppressed by Ptch. De-repression of Smo results in activation of Gli proteins by a mechanism involving

two major Gli inhibitors – Protein Kinase A (PKA) and Suppressor of Fused (SuFu). However, the steps of the pathway that transduce the signal from Smo to PKA and SuFu remain poorly understood.

The regulation of Shh signaling by PKA has been extensively studied. In the absence of signal, Gli proteins are directly phosphorylated by PKA [3], which results in their conversion into transcriptional repressors, and ultimately leads to abrogation of Shh target gene expression [4]. Conversely, inhibition of PKA activity results in the formation of transcriptional activator forms of Gli proteins, which leads to activation of Shh target genes [5,6]. These data suggest that PKA is required to maintain low baseline levels of Shh-dependent transcripts, but until recently little was known about the possible ways in which Shh might antagonize this inhibitory function of PKA. It has been hypothesized that Smo acts as a G-protein coupled receptor (GPCR) and inhibits PKA by inducing the G_i-family of heterotrimeric GTPases [7–9], but this view has been controversial [10,11]. The Smo–G_i link has later been suggested to represent a non-canonical branch of the pathway [12]. On the other hand, recent work shows that Smo regulates the subcellular localization of another GPCR, Gpr161, which turns out to be crucial for the canonical PKA-mediated inhibition of Gli protein function [13]. Regardless of the mode of regulation of the PKA–Gli interaction by Smo, there remains a major question of how Hh signaling can remain robust to changes in PKA activity caused by GPCRs utilizing G_{αs}, which positively couple to the adenylate cyclase (AC)/PKA pathway. Conversely, it is not clear if in some cases these GPCRs might be used to adjust Shh transcriptional response based on environmental cues.

Much recent interest in Shh signaling stems from the fact that this pathway is involved in a broad range of human cancers [14]. In

Abbreviations: 7-TM, seven transmembrane domain; AC, adenylate cyclase; AKAP, A-kinase anchoring protein; Bnz-cAMP, N6-benzoyl-cAMP; 8-CPT, 8-CPT-2-Me-cAMPs; cGCPs, cerebellar granule cell progenitors; IBMX, isobutylmethylxanthine; FSK, forskolin; GliA, Gli activator; GliR, Gli repressor; GPCR, G-protein coupled receptor; MB, medulloblastoma; PAC1 Fl, PAC1-expressing flp-in NIH/3T3 cells; PACAP, pituitary adenylate cyclase activating polypeptide; PKA, protein kinase A; PKC, protein kinase C; PI3K, phosphoinositide-3 kinase; Ptch, Patched; SDF-1, Stromal cell-derived factor 1; Shh, Sonic hedgehog; Shh-N, N-terminal fragment of Shh; Smo, Smoothened.

[☆] This is an open-access article distributed under the terms of the Creative Commons Attribution-NonCommercial-No Derivative Works License, which permits non-commercial use, distribution, and reproduction in any medium, provided the original author and source are credited.

^{*} Corresponding author at: Intellectual and Developmental Disabilities Research Center, The David Geffen School of Medicine, University of California, Los Angeles, Semel Institute for Neuroscience and Human Behavior, Neuroscience Research Building, Room 345, 635 Charles E. Young Drive South, Los Angeles, CA 90095-7332, United States. Tel.: +1 310 825 0179.

E-mail address: jwaschek@mednet.ucla.edu (J.A. Waschek).

particular, approximately 30% of cases of medulloblastoma, the most common pediatric brain tumor, are thought to be driven by germline and acquired genetic mutations in Shh pathway components [15,16]. Accordingly, mice harboring activating mutations of Smo or lacking a single copy of Ptch develop MB-like tumors [15]. These Shh-dependent MBs arise from a class of precursor cells known as cerebellar granule cell progenitors (cGCPs) [17], whose rapid postnatal proliferation is critically dependent on Shh secreted from the Purkinje cells of the cerebellum [15]. Various signals, including the extracellular matrix [18] and secreted peptides [19–21], cooperate with Shh to regulate the proliferation and differentiation of cGCPs. Failure of these mechanisms may contribute to uncontrolled proliferation of cGCPs, leading to the generation of MB tumors.

Our particular interest is in the role of pituitary adenylate cyclase-activating polypeptide (PACAP) in cGCP proliferation and MB tumorigenesis. PACAP is a short secreted polypeptide with ubiquitous expression and pleiotropic functions [22]. Both PACAP and its receptors are expressed in the cerebellum at the peak of cGCP proliferation [23–25] and PACAP can inhibit Shh-driven cGCP proliferation *in vitro* [26]. Importantly, we found that incidence of MB in mice lacking a single copy of Ptch is increased three fold by an additional heterozygous mutation in the gene encoding PACAP [27]. We hypothesized that the tumor suppressor role of PACAP in MB was due to a direct inhibitory effect of PACAP on Shh signaling in cGCPs. On the other hand, a recent study linked the antiproliferative effect of PACAP with the expression of the transcription factor Gli2 [28], suggesting that the effects of PACAP on cGCP proliferation are independent of Shh signaling. Further work was therefore necessary to resolve the controversy surrounding the mechanism of the antiproliferative action of PACAP in cerebellar development.

In the present work, we show that the inhibitory effects of PACAP on cGCP proliferation are mostly due to the direct effect of PACAP on Shh signaling. We further demonstrate that PACAP acts by inducing the activity of PKA, which leads to changes in subcellular localization of the transcription factor Gli2. Finally, we use the PACAP/Shh interaction to show that elevated total cellular PKA activity can coexist with moderately high levels of Shh signaling, which runs counter to the current views of Shh pathway regulation by PKA. We explain this apparent paradox by proposing a new model involving PKA activity compartmentalization. This model both explains the apparent robustness of the Shh signal in the face of PKA activity fluctuations, and shows how various GPCRs can serve to fine-tune the response of cells to the Shh ligand.

2. Material and methods

2.1. Culture of primary cGCPs

Primary cGCPs were isolated and cultured as detailed in Hatten et al. [29] with some modifications. Briefly, postnatal day 3 mouse pups were anesthetized with pentobarbital and sacrificed by decapitation. Cerebella were dissected in calcium and magnesium-free HBSS and meninges peeled off using fine tweezers. Cerebella were moved into a trypsin/DNase solution and minced. Following a 5-minute incubation at room temperature, the cell suspension was pelleted by centrifugation and the supernatant was replaced with cold DNase solution. The cells were gently dissociated by trituration with fire polished Pasteur pipettes and pelleted by centrifugation. The cells were resuspended in DNase solution and diluted with ice-cold HBSS. Granule cells were separated from cell debris and other cerebellar cells by centrifugation on a 35%/60% Percoll gradient, and the interface between the 35% and the 60% Percoll layers was collected. The cells were pelleted and then resuspended in culture media containing Neurobasal, penicillin/streptomycin/glutamine (Invitrogen, 1×), 1 mM sodium pyruvate, 0.04 µg/mL triiodothyronine, 0.1 mg/mL BSA, 0.04 µg/mL sodium selenite, 60 µg/mL N-acetylcysteine, 0.06 µg/mL progesterone, 5 µg/mL insulin, 100 µg/mL apo-transferrin, and 16 µg/mL putrescine. Purity of the cultures (90–95%) was ascertained by phase-

contrast microscopy, where cGCPs present a very characteristic morphology with small cytoplasm-poor cell bodies and multiple projections. In experiments using SDF-1 the media was supplemented with 20 mM KCl (final KCl concentration 25 mM), which was required for SDF-1 to have an effect on Shh signaling. Additional KCl did not impact the effects of Shh-N and PACAP. The cells were plated at 2.5×10^5 cells/cm² on poly-D-lysine (0.01%) coated 4-well culture dishes (Nunc), and treated as described. The treatment time was 2 h for western blot analysis and 6 h for RT-PCR, unless otherwise indicated.

2.2. [³H]-thymidine incorporation

cGCPs were isolated as above and plated at 3×10^5 cells/cm² on poly-D-lysine coated 96-well culture dishes (Nunc). The cells were grown in the presence or absence of drugs for 24 h and [³H]-thymidine (1 µCi/well) was added during the last 6 h of incubation. DNA was precipitated for 30 min using 5% trichloroacetic acid, washed with PBS, resolubilized using 0.5 M NaOH/0.5% SDS, transferred into scintillation liquid (Econo-Safe, RPI) and incorporated radioactivity was counted on a liquid scintillation counter (Beckman).

2.3. RNA extraction and real-time quantitative RT-PCR

RNA was extracted from CB GCP cultures with the TRIzol reagent (Invitrogen) following the manufacturer's instructions. In order to aid RNA pellet visualization glycogen (1 mg) was added to each sample. cDNA was generated using the iScript cDNA synthesis kit (Bio-Rad) and quantitative PCR was performed using the iQ SYBR green supermix (Bio-Rad). The results were analyzed using the standard curve method with GAPDH used as the housekeeping gene. Primers used for qPCR were as follows: GAPDH: forward – ggccttccgtgttctctac, reverse – tgtcatcacttggcagggtt, Gli1: forward – atctcttcttctctctctcc, reverse – cgaggctggcatcagaa, mycN: forward – ggatgatctgcaagaaccag, reverse – gtcatctcttccgggtagaa, ccnd1: forward – tgccgaaatctgtggc, reverse – aggaagcgggtccaggtagttc, Ptch1: forward – agagcgaagttc agagactc, reverse – aatatgaggagaccacaac. Each set of primers was validated by cloning and sequencing of the PCR product.

2.4. Microarray analysis

cGCPs were cultured as detailed above and treated for 6 h with or without Shh-N (1 µg/mL), PACAP (10 nM), or both. RNA extracted from each treatment was pooled from at least 6 samples per experiment and from 3 to 4 independent experiments. Three samples for each treatment group were generated in this way. Each RNA sample was processed for microarray hybridization at the UCLA DNA Microarray Core and the generated cDNA was hybridized to the Affymetrix GeneChip Mouse Genome 430 2.0 microarray. Results were processed using the Affymetrix Expression Console using thePLIER algorithm for conversion of raw data into expression values.

2.5. Generation and culture of PAC1-expressing NIH/3T3 flp-in cells (PAC1 FI)

Stable cell lines expressing low levels of the PAC1 receptor were generated using the flp-in system (Life Technologies). Briefly, the PAC1 receptor (the short/null variant) was cloned from the adult mouse brain cDNA by means of PCR amplification and ligation into the pENTR2B plasmid. The insert was transferred into the pEF5/FRT/V5-DEST plasmid by Gateway cloning. NIH/3T3 flp-in cells (Life Technologies) were co-transfected with the pOG44 and the pEF5/FRT/V5-DEST-PAC1 plasmids, and stable integrants were selected using hygromycin. The cells were cultured in media containing high-glucose DMEM, sodium pyruvate, Gluta-MAX, MEM non-essential amino acids, penicillin/streptomycin,

and 10% fetal bovine serum (FBS). 18–36 h before the experiment, the cells were serum-starved in media containing 0.5% FBS.

2.6. Protein extraction and western blot analysis

Proteins were extracted from cell cultures with NP-40 lysis buffer containing protease and phosphatase inhibitors. Total protein was quantified using the detergent resistant Bio-Rad protein assay (Lowry) and equal protein samples were resolved by SDS-PAGE electrophoresis. Protein was transferred onto PVDF or nitrocellulose membranes and equal loading was ascertained by Ponceau S staining. The membranes were blotted with the following antibodies: anti-phospho-PKA substrates (Cell Signaling #9624), anti phospho-PKC substrates (Cell Signaling #2261) anti-ERK and anti-phospho-ERK, anti-MEK1/2 and anti-phospho-MEK1/2 (all from Cell Signaling). Chemiluminescent detection was performed using secondary antibodies coupled to HRP and ECL or ECL + substrates (GE Healthcare) and Kodak BioMax Light film. For experiments on PAC1 FI cells the primary antibodies used were: anti-Gli1 (Cell Signaling #2643), guinea pig anti-Gli2 (kindly provided by Dr. Rajat Rohatgi), anti-lamin A (abcam), anti- α -tubulin (Sigma). For these experiments, secondary antibodies were coupled to IRDye fluorophores and the membranes were imaged on the Li-Cor Odyssey apparatus.

2.7. Immunofluorescence

PAC1 FI cells were cultured on round glass coverslips. They were starved in media containing 0.5% FBS for 24 h, and then treated for 2 h with the indicated drugs. The cells were fixed in 4% paraformaldehyde for 10 min, and then permeabilized/blocked in blocking solution (PBS + 0.1% Triton X-100, 1% normal donkey serum, 1% BSA) for 30 min. Primary and secondary antibodies were diluted in blocking solution. Primary antibody incubation was 1 h at room temperature, and secondary antibody incubation was 30 min at room temperature. Both antibody incubations were followed by 3×5 min wash in PBS + 0.1% Triton X-100. The coverslips were mounted on microscope slides using the ProLong Gold mounting media with DAPI. The cells were imaged on the Leica SP5 confocal microscope and stacks of 10 confocal slices were taken for each image, which were subsequently flattened by maximum intensity projection. For unsupervised quantification of ciliary tip fluorescence, a custom-made Jython script was used in the Fiji software suite.

2.8. Nuclear-cytoplasmic fractionation

Nuclear-cytoplasmic fractionation was performed as described previously [30].

2.9. Statistical data analysis

Statistical data analysis was performed in Microsoft Excel using specialized worksheets to calculate p values for Student *t*-test. Graphs were plotted using R. Error bars on all charts represent standard deviation of 4–10 measurements of independent samples.

2.10. Chemicals

PACAP-38 (referred to as “PACAP” throughout the text), and other drugs were purchased from Calbiochem, unless otherwise indicated. Shh-N (mouse, recombinant) was purchased from R&D. Mouse SDF-1 α was purchased from Peprotech. Forskolin was purchased from Sigma. SAG was purchased from Axxora.

3. Results

3.1. PACAP antagonizes Shh-driven proliferation of cGCPs and Hh target gene expression

We previously reported that PACAP antagonizes Shh-driven BrdU incorporation into cultured cGCPs [26]. Similarly, we found here that [³H]-thymidine incorporation into the DNA of cGCPs is increased by treatment with the Shh N-terminal fragment (Shh-N) (1 μ g/mL) and that this increase is attenuated by treatment with 10 nM PACAP (Fig. 1A). In order to determine if the effect of PACAP on cGCPs might result specifically from the inhibition of Shh pathway rather than from a direct effect on proliferation, we performed DNA microarray analysis on mRNA from cGCPs treated for 6 h with Shh-N (1 μ g/mL), PACAP (10 nM), or both. In Shh-N-treated cells PACAP downregulates multiple direct and indirect Shh target genes (Fig. 1C) including Gli1 and Ptch1, two universal markers of Hh pathway activation, and cyclin D1, a known Hh effector gene that drives cGCP proliferation. Of all the genes upregulated more than 1.5-fold by treatment with Shh-N (98 probesets), 33% (32 probesets) were significantly ($p < 0.05$) downregulated and none (0%) are significantly upregulated by the addition of PACAP ($n = 3$ samples for each group). In contrast, of the 112 probesets upregulated more than 1.5-fold by PACAP treatment, none (0%) were significantly up- or downregulated by the addition of Shh-N (Fig. 1B, Supplementary Table 1B). This suggests that the antiproliferative effect of PACAP depends to a large degree on its ability to inhibit Shh signaling as opposed to a more general induction of genes that arrest proliferation. PACAP antagonizes the Shh-mediated induction of Gli1 gene expression in the presence of protein synthesis inhibitor cycloheximide, suggesting that the effect of PACAP on Shh signaling is direct, and not mediated through the transcription of additional PACAP target genes (Fig. 1D).

3.2. PACAP regulates the Shh pathway through PKA

To further understand the mechanism of PACAP-mediated inhibition of Shh signaling, we used phospho-specific antibodies to test what signaling pathways were activated in cGCPs in response to PACAP treatment. PACAP is known to activate the AC/PKA pathway, the DAG/IP₃/protein kinase C (PKC) pathway, the ERK pathway, and phosphoinositide-3 kinase (PI3K) signaling [22,31,32]. We found that in cGCPs PACAP does not appear to have an effect on MEK1/2 activity, but that it stimulates the phosphorylation of substrates of PKA, PKC and PI3K (Figs. 2A, S1A). Inhibition of PKC and PI3K has no effect on the ability of PACAP to block Shh-mediated Gli1 production, suggesting that these two kinases don't participate in the Shh-PACAP interaction in cGCPs (Fig. 2B). That left PKA as the most plausible mediator of the inhibition of Shh signaling by PACAP. Accordingly, the dose-response of the effect of PACAP on PKA activity closely parallels that of its effect on Gli1 production (Fig. 1A). To provide further evidence that PKA activation is involved in the inhibitory effect of PACAP on cGCPs, we tested other pharmacological activators of the AC/PKA pathway for their ability to inhibit Gli1 production in cGCPs. Indeed, forskolin, an AC activator, and N6-benzoyl-cAMP, a direct selective activator of PKA, both mimic the effect of PACAP on Gli1 gene expression (Fig. 2C).

AC/cAMP signaling, in addition to stimulating PKA, also activates a class of guanidine nucleotide exchange factors known as cAMP-GEFs. In fact PACAP was shown to induce cAMP-GEF activity in hippocampal neurons [33]. In order to rule out the involvement of cAMP-GEFs in PACAP-mediated inhibition of the Shh pathway, we co-treated cGCPs with Shh and the cAMP-GEF activator 8-CPT-2-Me-cAMPS. This compound, used at doses known to be sufficient for cAMP-GEF activation, failed to block Shh-induced Gli1 expression, suggesting that cAMP-GEF activation by PACAP is not sufficient for its effects on Shh signaling in cGCPs (Fig. 2D).

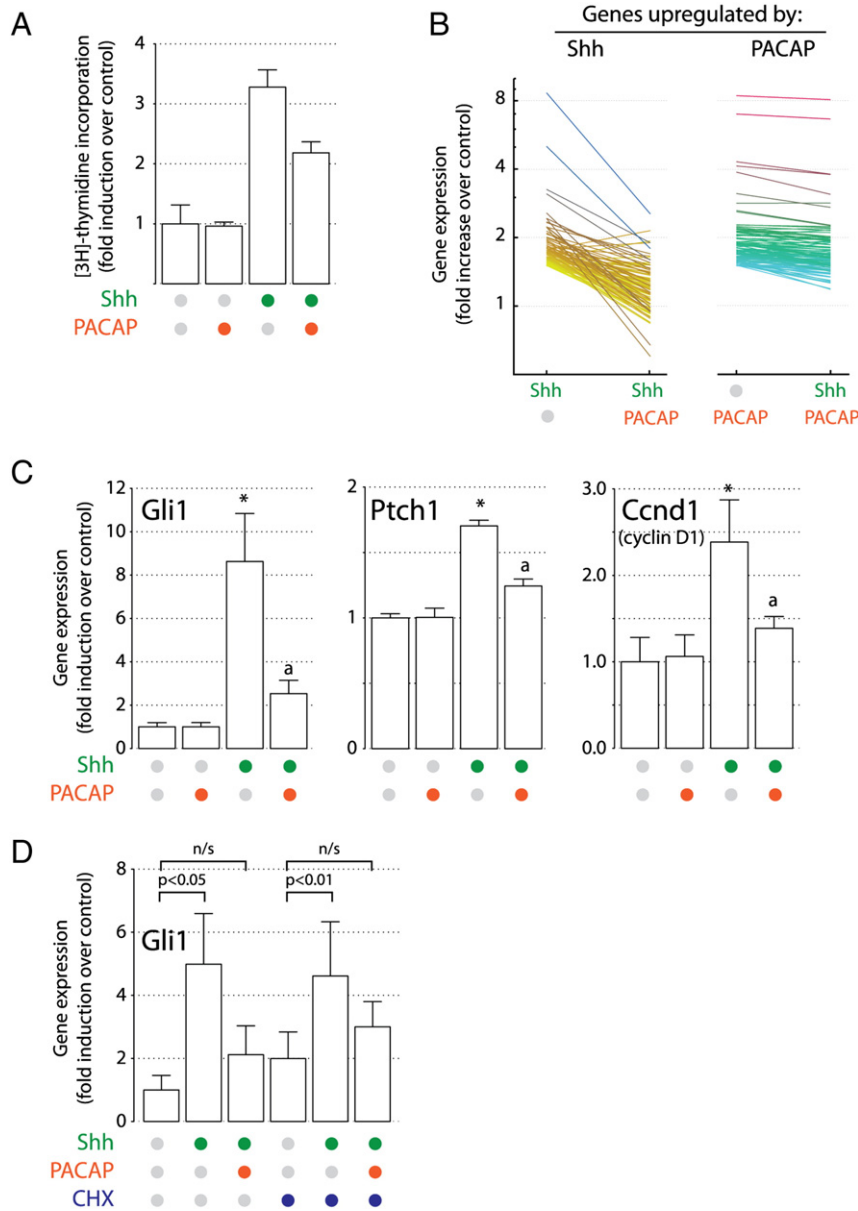


Fig. 1. PACAP antagonizes Shh-driven cGCP proliferation and target gene expression. (A) Cell proliferation was measured by [³H]thymidine incorporation in cGCPs cultured for 24 h in defined media supplemented with Shh-N (1 μg/mL), PACAP (10 nM) or both. (B, C) cGCPs were cultured for 6 h in defined media in the presence or absence of Shh-N (1 μg/mL) and/or PACAP (10 nM). RNA was isolated from the cells and subjected to GeneChip analysis. (B) Left panel shows all probesets upregulated at least 1.5-fold by Shh-N and right panel shows all probesets upregulated at least 1.5-fold by PACAP. Individual lines represent probesets. Colors were assigned arbitrarily and are related to the degree of upregulation of gene expression by Shh-N (left) or PACAP (right). (C) Expression of individual known Shh target genes Gli1, Ptch1, and cyclin D1 (Cnd1) was analyzed as above. * – p < 0.05 relative to control, a – p < 0.05 relative to Shh alone. (D) cGCPs were cultured for 30 min in the presence or absence of 10 μg/mL cycloheximide (CHX), and then Shh-N and/or PACAP was added to the culture media for additional 6 h. Gli1 expression was assayed by quantitative RT-PCR.

3.3. PKA inhibition induces Shh signaling independently of Shh-N in cGCPs

Since PACAP appears to blocks Shh signaling through induction of PKA, we hypothesized that inhibition of PKA would stimulate Shh target genes in cGCPs. Such effects have previously been observed in the developing spinal cord [5,6] and in mouse embryonic fibroblasts [34]. Treatment of cGCPs with the PKA inhibitor H89 (10–30 μM) caused a dose-dependent increase in Gli1 expression (Fig. 3A) and a correlated reduction in PKA activity (Fig. 3B). At the highest dose used (30 μM) H89 induces Gli1 expression to the same extent as Shh-N (1 μg/mL) and the combination of Shh-N plus H89 does not produce any further increase in Gli1 mRNA levels over that induced by either drug alone. Consistent with the hypothesis that PACAP acts on Shh signaling through PKA induction, PACAP does not abrogate H89-induced increase in Gli1 expression (Fig. 3C). Also, two other PKA inhibitors,

PKI and Rp-cAMPS, induce Gli1 production in cGCPs, albeit less effectively than H89 (Fig. 3D). These data provide evidence for the essential role of PKA in repressing Shh target gene expression in the absence of signal, but do not explain how this baseline PKA activity is maintained in the absence of Shh and PACAP.

3.4. SDF-1 signaling through G_{αi} amplifies Shh-N response to induce Gli1 expression

GPCRs can regulate AC activity in two ways: receptors coupled to G_{αs}, such as the PACAP receptor, activate AC, whereas receptors that bind G_{αi} block AC and act as inhibitors of PKA activity. Thus, G_{αi}-coupled receptor stimulation should mimic the effect of pharmacological inhibition of PKA. cGCPs express CXCR4, a G_{αi}-coupled 7-TM receptor that binds SDF-1, a peptide secreted by the pia matter of the cerebellum

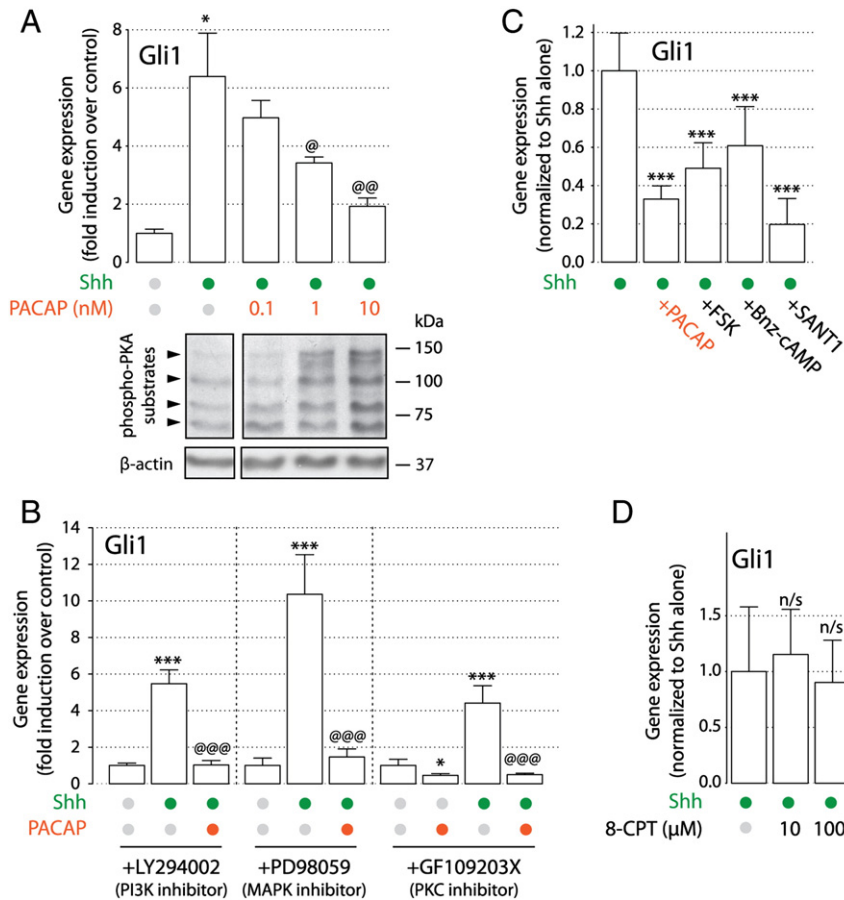


Fig. 2. PACAP regulates Gli1 gene expression dose-dependently by induction of PKA. (A) cGCPs were cultured in the presence of indicated doses of peptides and drugs. Gli1 RT-PCR was performed on RNA isolated after 6 h of treatment. Western blots were performed on protein isolated after 2 h of treatment. The effect of PACAP on Shh-N-induced Gli1 gene expression is shown in the top panel, and phosphorylation of PKA target proteins under the same conditions is shown in the bottom panel; ** – $p < 0.01$ relative to control, @ – $p < 0.05$ relative to Shh alone, @@ – $p < 0.01$ relative to Shh alone (B) cGCPs were pretreated for 30 min with inhibitors of PKC (GF109203X; 5 μ M), MAPK1/2 (PD98059; 25 μ M), and PI3K (LY294002; 10 μ M), and then treated with Shh-N (1 μ g/mL), PACAP (10 nM) or both for 6 h in the presence of the inhibitor. Gli1 gene expression was assayed by quantitative RT-PCR; * – $p < 0.05$, and *** – $p < 0.001$ relative to kinase inhibitor alone, @@@ – $p < 0.001$ relative to Shh + kinase inhibitor. (C, D) cGCPs were pretreated for 30 min with the AC activator forskolin (FSK; 5 μ M), specific activator of PKA N6-benzoyl-cAMP (Bnz-cAMP; 300 μ M), and a Smo antagonist SANT-1 (1 μ M) (C) or the cAMP-GEF activator 8-CPT-2-Me-cAMPS (8-CPT; D) and then treated for 6 h with Shh-N. Gli1 gene expression was measured as in (A). n/s – non-significant relative to Shh alone, *** – $p < 0.001$ relative to Shh alone.

and involved in cGCP development. SDF-1 has been shown to enhance proliferation of cGCPs in the presence of Shh-N in a pertussis toxin (PTX)-sensitive manner [21]. We hypothesized that SDF-1 exerts its effect on cGCP proliferation by enhancing Shh signaling through PKA inhibition. Indeed, even though SDF-1 does not have a significant effect on Gli1 expression either in the complete absence of Shh-N or in the presence of a saturating dose of Shh-N, it nevertheless amplifies the response to a suboptimal dose (0.03 μ g/mL) of Shh-N (Fig. 3E). However, in contrast to PACAP, we were unable to show a direct effect of SDF-1 on PKA activity (Fig. S2). This may reflect the fact that SDF-1 blocks PKA only very weakly – enough to significantly affect Gli1 mRNA levels, but not enough to be discernible by semi-quantitative blotting for phospho-PKA substrates. The ability of SDF-1 to enhance the effects of Shh-N in cGCP is further evidence that the G-protein/AC/PKA pathway plays a critical role in modulating the response of cGCPs to the Shh signal.

3.5. Shh target gene expression is not inversely correlated with total PKA activity

The currently predominant paradigm of Shh signaling assumes that PKA activity must be abrogated in order for the Shh pathway to be activated [30,35,36]. Our results showing an increase in Gli1 expression in cells treated with a PKA inhibitor (Fig. 2A) seem to corroborate this model. We therefore expected Shh-N to be able to have a negative effect on the phosphorylation of PKA substrates in cGCPs. Surprisingly, we

found no evidence of Shh-N affecting PKA activity (Fig. 4A). Also, PKA activity in untreated cells is barely detectable, as opposed to that in cells treated with PACAP (Figs. 2A, 4B). This raised the question of how target gene expression is kept silent in the absence of Shh. We hypothesized that only a small pool of PKA is under the direct control of Shh and that this pool is sufficient to keep the pathway in the off state in untreated cells. If that were the case, we would expect that under some circumstances high levels of Shh signal might coexist in the same cell with activated PKA, as long as PKA activation was limited to a Shh-independent pool of PKA. In order to test this assumption, we co-treated cGCPs with Shh-N and a low dose (1 nM) of PACAP. Strikingly, in these cells both Gli1 and total cellular PKA activity are significantly higher than in control cells (Fig. 4B), providing strong evidence for the partial independence of Shh signaling from the pool of PKA activated by PACAP. In summary, the relationship between total cellular PKA activity and Shh signaling is not a simple inverse correlation. Instead, a new model involving compartmentalization of PKA activity seems to be most consistent with our data.

One concern with these data was that the observed discrepancy between activation of global PKA activity and inhibition of Shh signaling could be due to cell-to-cell differences in our primary cultures. For example, one could imagine that the cells that expressed Gli1 were not the same as cells in which PACAP induced PKA activity. In order to address this issue, we established a stable NIH/3T3 fibroblast flp-in cell line expressing low levels of the mouse PAC1 receptor from a single

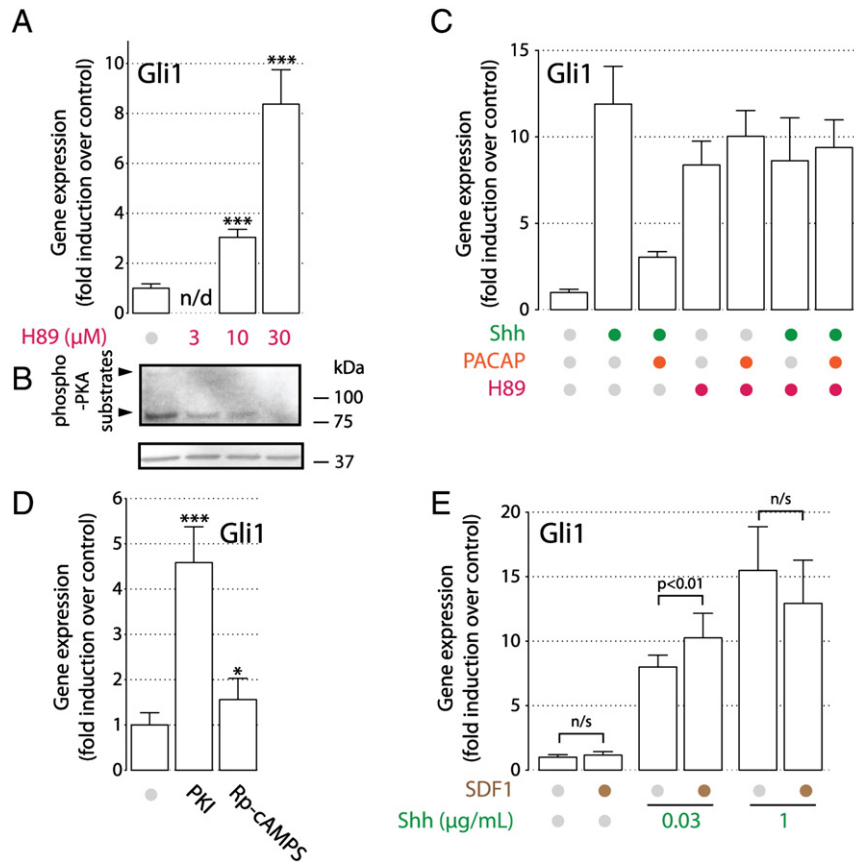


Fig. 3. PKA inhibition induces Hh target gene expression. (A) cGCPs were treated for 6 h with indicated doses of H89. Gli1 RT-PCR was performed on isolated RNA. *** – $p < 0.001$ relative to control, n/d – no data. (B) Anti-phospho-PKA-substrate western blot of samples treated with H89 (doses as in (A) above) or vehicle (DMSO) for 2 h. (C) cGCPs were pretreated for 30 min with 30 μ M H89, then treated for 6 h with 1 μ g/mL Shh-N, 10 nM PACAP, or both in the presence of H89. (D) cGCPs were treated for 6 h with PKA inhibitors PKI (10 μ M) and Rp-cAMPS (250 μ M). Experiment was performed as in (A) * – $p < 0.05$, *** – $p < 0.001$ relative to control. (E) SDF-1 synergizes with Shh. cGCPs were cultured for 6 h in defined media in the presence of 25 mM KCl with the addition SDF-1 (1 μ g/mL) and/or Shh-N at indicated doses. Gli1 expression was analyzed by RT-PCR.

defined locus in the genome (PAC1 FI cells). In these cells the Smo agonist SAG induced Gli1 protein expression, and PACAP antagonized this effect in a dose-dependent manner (Fig. 5A). Similarly to what we observed with Shh pathway activation in cGCPs, SAG failed to decrease global levels of PKA-mediated phosphorylation (Fig. 5B). Moreover, increase of PKA target protein phosphorylation induced by 1–10 nM PACAP could not fully counteract the effect of SAG on Gli1 production, while a high dose of PACAP (100 nM) completely abrogated Gli1 upregulation by SAG (Fig. 5A). This is consistent with what we observed in cGCPs, suggesting that our earlier observations (Fig. 4B) are not explained by heterogeneity in primary cGCP cultures.

3.6. Gli2 trafficking is partially insensitive to global PKA activity

To further explore the molecular mechanisms of the interaction between PACAP and Shh, we investigated how PACAP affected the trafficking of Gli proteins. Gli1 was not an appropriate protein to study in this context, because it is mostly regulated at the level of transcription. Instead, we examined subcellular localization of Gli2, whose expression does not change upon SAG treatment, and which instead is regulated directly by posttranslational modifications and intracellular trafficking. Upon Hh pathway activation, Gli2 accumulates at the tip of the primary cilium, a small microtubule-based protrusion of the cell membrane known to be essential for Hh signaling [37]. This ciliary trafficking step is hypothesized to be necessary for the subsequent nuclear translocation of Gli2, and for Gli2-mediated transcriptional activation of target genes [30,36]. Accordingly, SAG treatment induces a strong accumulation of Gli2 at tips of primary cilia (Fig. 5C) and in the nuclei (Fig. 5B) of PAC1 FI cells. Importantly, neither SAG-mediated ciliary accumulation, nor

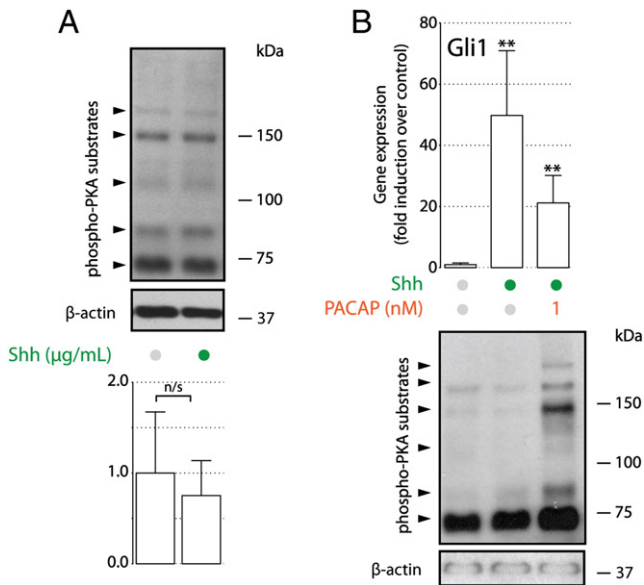


Fig. 4. Gli1 expression is partially independent of global PKA activity. cGCPs were cultured in defined media in the presence of indicated concentrations of PACAP and Shh-N for 6 h (for RT-PCR) or 2 h (for western blot). (A) Anti-phospho-PKA substrate western blot was performed on protein isolated from cGCP samples. (B) RT-PCR was performed on RNA isolated from cGCPs (top panel) and anti-phospho-PKA western blot was performed on protein from corresponding samples (bottom panel).

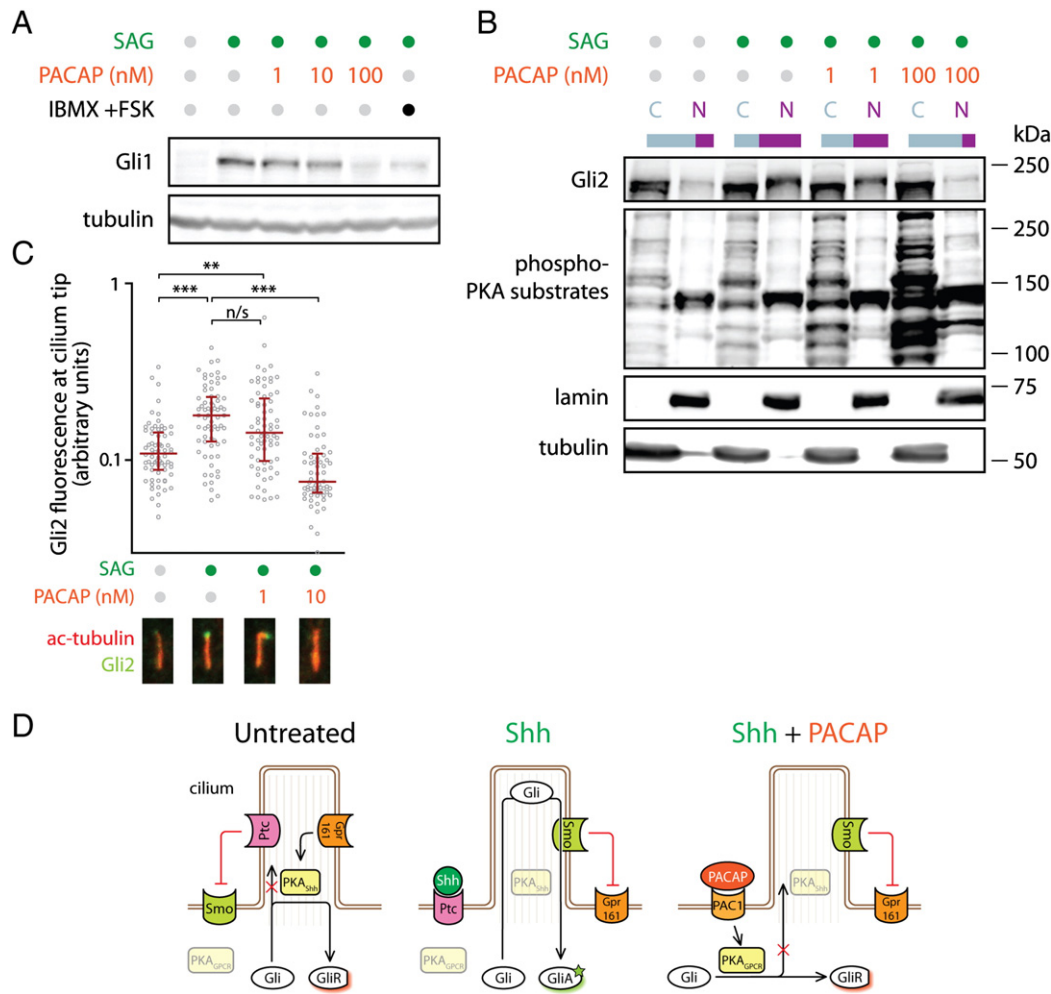


Fig. 5. Subcellular localization of Gli2 is partially independent of total cellular PKA activity in FI cells stably-transfected with PAC1. (A) PAC1 FI cells were treated for 24 h with SAG (100 nM), with or without PACAP or IBMX (100 μ M) + FSK (0.1 μ M). Gli1 western blot was and Gli1 expression was quantified by western blot. (B) PAC1 FI cells were treated for 2 h with SAG (100 nM) and PACAP (1–100 nM), as indicated. The cells were fractionated to separate nuclei from the cytoplasm and each fraction was blotted separately. Tubulin and lamin are only present in the cytoplasm and nuclei, respectively. “C” – cytoplasmic fraction, “N” – nuclear fraction, gray and purple bars represent, respectively, the relative abundance of Gli2 in the cytoplasmic and nuclear fractions. (C) PAC1 FI cells were treated for 4 h with SAG (100 nM) and PACAP (1–10 nM) were indicated. The cells were fixed and stained with anti-Gli2 and anti-acetylated-tubulin antibodies, and imaged on a confocal microscope. Gli2 fluorescence at the cilium tip was quantified for $n = 64$ –70 cells from at least 3 separate fields of view. Each gray circle represents a single cilium and bars represent median \pm 95% confidence interval on a log scale of fluorescence intensity. Images below the chart show a representative cilium for each treatment group; ** – $p < 0.01$, *** – $p < 0.001$, n/s – not significant. (D) The “two brake” model of the interplay between the Shh pathway and PKA-mediated signaling. Left panel: in the absence of Shh, PKA_{Shh} is activated by Gpr161 and prevents Gli protein translocation into the primary cilium, ultimately resulting in their conversion into transcriptional repressors (GliR). Middle panel: in Shh-treated cells, Smo enters the cilium, which causes Gpr161 to exit the cilium and abrogates PKA_{Shh} activity. Gli proteins accumulate in tips of cilia and are converted into transcriptional activators (GliA). Right panel: in cells treated with Shh and PACAP, PKA_{Shh} remains off, and instead a second pool of PKA, PKA_{GPCR} becomes activated by the PACAP receptor PAC1. If PKA_{GPCR} activity is sufficiently high, it will block Gli ciliary translocation and stimulate GliR formation. See the Discussion section for a detailed explanation.

SAG-induced nuclear translocation of Gli2 is abrogated by co-treatment with 1 nM PACAP, a dose that significantly increases phosphorylation of PKA substrates (Fig. 5B, C). In contrast, higher doses of PACAP (10–100 nM) completely abolish SAG-induced changes in Gli2 localization. These results are consistent with the effects of PACAP on Gli1 production in both cGCP and PAC1 FI cells, and demonstrate that the paradigm of the antagonism between cellular PKA and Shh signaling needs to be refined.

4. Discussion

Protein kinase A is a major inhibitor of Shh signaling. It is now well established that loss of PKA signaling is sufficient to activate transcription from Shh-sensitive promoters almost to the same extent as the binding of Shh to Ptch [5,6,34] (Fig. 3B). This data suggests that PKA belongs to the core Shh signaling, lying at a step downstream of Smo and upstream of Gli transcription factors. In the simplest model Smo would repress PKA activity, which in turn would repress Gli proteins. A simple

sequential repression model, however, requires that the baseline PKA activity be high, so that Gli proteins can be kept inactive in the absence of treatment. This is not consistent with our observations, since the two Shh-responsive cell types that we tested had barely detectable baseline PKA phosphorylation (Figs. 2A, 5B). This is not surprising, since maintaining high PKA activity constantly in all Shh-responsive cells would be energetically costly and would likely result in non-specific phosphorylation of substrates belonging to other signaling pathways. Another flaw of the sequential repression model is that cells could not maintain robust responses to Shh given their highly variable complement of GPCRs, each of which could in principle affect global PKA levels.

Our study shows for the first time that high Shh signal can be maintained despite large variations in total cellular PKA activity (Fig. 4B). We also demonstrate that high overall levels of PKA-mediated phosphorylation are not required to keep Shh signaling silent. The most parsimonious way to explain this paradoxical uncoupling of Shh signaling from PKA activity is to suggest that two pools of PKA

exist in each cell (Fig. 5D). The first small pool, PKA_{Shh}, is controlled by Shh signaling and is turned on in untreated cells. This pool is sufficient to shut down signaling in the absence of Shh ligand, most likely because it co-localizes well with Gli proteins, which are its primary effectors. Since Gli proteins characteristically undergo trafficking to primary cilia, it is tempting to speculate that PKA_{Shh} is localized in the periciliary region. Consistent with that claim, PKA accumulation at the base of primary cilia has been shown previously through the use of FRET-based sensors and has been stipulated to play a role in Shh signaling in cGCPs and in the developing spinal cord [6,35]. PKA is maintained at the base of cilia by interacting with protein scaffolds known as AKAPs anchored at the basal body, and inhibition of this interaction by the cell-permeable peptide St-Ht31 abolishes Shh-mediated proliferation in cGCPs [35]. Phosphodiesterases (PDE), which accompany PKA on AKAP scaffolds and serve to limit the area of high cAMP concentration, also appear to play a role in Shh signaling. Treatment of NIH/3T3 cells with the cAMP PDE inhibitor IBMX significantly reduced SAG-mediated Gli1 production (Fig. S3).

How might cells maintain the high localized PKA activity at the cilium base? It has recently been discovered that a ciliary G_s-coupled receptor Gpr161 is crucial for Shh signaling inhibition at baseline [13]. This receptor, acting through the AC/PKA cascade could well be responsible for maintaining high baseline activity of PKA_{Shh}. Its exit from the cilium upon stimulation of Smo might constitute a plausible mechanism for Shh-mediated abrogation of PKA_{Shh} activity.

The second of the two putative PKA pools, which we will refer to as PKA_{GPCR}, is mostly inactive in the absence of cognate ligands. It is not concentrated at the cilium and responds to stimulation by GPCRs distributed throughout the plasma membrane, such as the PACAP and SDF-1 receptors. Its moderate activation by GPCR ligands does not fully abrogate Shh signaling, but high levels of PKA_{GPCR} activity are still sufficient to phosphorylate, and thus inhibit, most Gli proteins.

What results from the interplay of the two PKA pools is a model not unlike a “two brake” system in an automobile. PKA_{Shh} constitutes the “parking brake”, which must be released in order for Shh signaling to commence. PKA_{GPCR} is the “foot brake pedal”, which can adjust the levels of signaling or even completely stop the pathway if pressed sufficiently hard.

What makes the “two brake” model operate is the localization of Gli proteins to primary cilia, where they interact with PKA_{Shh}. Interestingly, we show that ciliary accumulation of Gli proteins is itself regulated by both Shh signaling and by PACAP (Fig. 5C). We believe that the inhibition of ciliary transport of Glis by PACAP is mediated through the AC/PKA pathway. Stimulation of AC by FSK has been previously shown to abrogate Gli ciliary accumulation, but this effect was assumed to be non-specific, since it persisted in cells lacking all major α and β catalytic subunits of PKA [6]. In contrast, we show that a similar effect can be achieved through physiological induction of the AC/PKA pathway by PACAP. Two possible explanations of the discrepancy can be advanced. The effect of PACAP and FSK on Gli localization could be mediated through AC but independently of PKA, and therefore would be preserved in PKA mutant mice. Alternatively, the inhibitory effect of FSK in PKA mutant cells could have been mediated by the γ catalytic subunit of PKA [38], which, although not normally strongly expressed in the neural tube, could have become amplified in mutant mice as a compensatory mechanism. We favor the latter explanation, because transient inhibition of PKA by PKI, which cannot induce compensation, is sufficient to stimulate Gli accumulation at cilia (P.N., unpublished data). In conclusion, we believe that PACAP regulates Shh signaling through the AC/PKA cascade by affecting the intracellular trafficking of Gli proteins to the primary cilium.

Interestingly, Hh signal transduction seems to have diverged significantly between mammals and *Drosophila*. Not only are cilia dispensable for Hh signaling in the fly, but also Smo appears to act in this species as a *bona fide* G_i-coupled receptor, regulating intracellular cAMP and thus able to affect global PKA activity [8]. Direct G_i coupling also seems to

be essential for non-canonical Gli-independent induction of Rho small GTPases by Smo. Importantly, Rho induction by Smo is preserved in a ciliary-localization deficient variant of Smo, stressing the independence of G_i-linkage of Smo of its ciliary localization [12]. Therefore, the “two brake” system appears to be a characteristic feature of only the canonical, cilium-dependent vertebrate Hh signaling, perhaps reflecting its adaptation to a diverse set of functions played by this pathway in vertebrate development.

One example of the utility of the “two brake” system is the role it plays in blocking Shh-pathway-dependent tumorigenesis during cerebellar development. Deletion of one copy of Ptch effectively damages the “parking brake” PKA_{Shh} pool in the neonatal cerebellum, leading to MB formation in mutant mice [39]. In these mice PKA_{GPCR} is the only pool that can stop excessive proliferation. Additional mutation of PACAP makes this “brake pedal” PKA pool less effective, thus leading to increased incidence and aggressiveness of the tumors [27]. Importantly, PKA_{GPCR} should remain intact in most Shh-driven malignancies, which makes it possible to inhibit Shh-dependent tumorigenesis by treatment with an appropriate GPCR ligand, such as PACAP [27,40]. An even more attractive therapeutic approach would be to prevent the aberrant Shh signal from releasing the “parking brake”. Some important insights into the regulation of this PKA pool have recently been provided [6,9,13,35], but a therapeutically exploitable strategy to target PKA_{Shh} remains to be devised. Our study should be a valuable stepping stone toward that goal.

5. Conclusions

- PACAP blocks Shh signaling through PKA inhibition.
- Shh affects Gli protein localization and target gene transcription by regulating a compartmentalized pool of PKA.
- The interplay between PACAP- and Shh-controlled PKA pools results in fine-tuning of the Shh-induced transcriptional program and plays a role in cerebellar development and disease.

Supplementary data to this article can be found online at <http://dx.doi.org/10.1016/j.cellsig.2013.07.012>.

Author's contributions

P.N. and J.W. conceived the study, designed the experiments, analyzed the data, and wrote the manuscript. P.N. conducted experiments. A.Z. and M.Y. conducted experiments on cGCPs under the supervision of P.N. and J.W.

Acknowledgment

The authors would like to thank Dr. Cristina Ghiani, Dr. Vincent Lelievre, Akop Seksenyan, Dr. Joseph Cohen, Dr. Rajat Rohatgi, and Dr. Matthew Scott for helpful discussions. We also thank Dr. Rohatgi for supplying the anti-Gli2 antibody. This work was supported by the National Brain Tumor Society grant 9280; and the following NIH grants: CA110384, HD34475, HD04612, and HD068686.

References

- [1] A.A. Merchant, W. Matsui, *Clinical Cancer Research* 16 (2010) 3130–3140.
- [2] T. Østerlund, P. Kogerman, *Trends in Cell Biology* 16 (2006) 176–180.
- [3] B. Wang, J.F. Fallon, P.A. Beachy, *Cell* 100 (2000) 423–434.
- [4] D. Tempe, M. Casas, S. Karaz, M.-F. Blanchet-Tournier, J.-P. Concordet, *Molecular and Cellular Biology* 26 (2006) 4316–4326.
- [5] D.J. Epstein, E. Marti, M.P. Scott, A.P. McMahon, *Development (Cambridge, England)* 122 (1996) 2885–2894.
- [6] M. Tuson, M. He, K.V. Anderson, *Development (Cambridge, England)* 138 (2011) 4921–4930.
- [7] N.A. Riobo, B. Saucy, C. Dilizio, D.R. Manning, *Proceedings of the National Academy of Sciences of the United States of America* 103 (2006) 12607–12612.
- [8] S.K. Ogden, D.L. Fei, N.S. Schilling, Y.F. Ahmed, J. Hwa, D.J. Robbins, *Nature* 456 (2008) 967–970.

- [9] M. Barzi, D. Kostrz, A. Menendez, S. Pons, *The Journal of Biological Chemistry* 286 (2011) 8067–8074.
- [10] M. Hammerschmidt, A.P. McMahon, *Developments in Biologicals* 194 (1998) 166–171.
- [11] W.-C. Low, C. Wang, Y. Pan, X.-Y. Huang, J.K. Chen, B. Wang, *Developments in Biologicals* 321 (2008) 188–196.
- [12] A.H. Polizio, P. Chinchilla, L. Chen, S. Kim, D.R. Manning, N.A. Riobo, *The Journal of Biological Chemistry* 286 (2011) 19589–19596.
- [13] S. Mukhopadhyay, X. Wen, N. Ratti, A. Loktev, L. Rangell, S.J. Scales, P.K. Jackson, *Cell* 152 (2013) 210–223.
- [14] K.D. Marini, B.J. Payne, D.N. Watkins, L.G. Martelotto, *Growth Factors (Chur, Switzerland)* 29 (2011) 221–234.
- [15] M.E. Hatten, M.F. Roussel, *Trends in Neurosciences* 34 (2011) 134–142.
- [16] T.S. Surawicz, B.J. McCarthy, V. Kupelian, P.J. Jukich, J.M. Bruner, F.G. Davis, *Neuro-Oncology* 1 (1999) 14–25.
- [17] R.J. Gilbertson, D.W. Ellison, *Annual Review of Pathology* 3 (2008) 341–365.
- [18] S. Blaess, D. Graus-Porta, R. Belvindrah, R. Radakovits, S. Pons, A. Littlewood-Evans, M. Senften, H. Guo, Y. Li, J.H. Miner, L.F. Reichardt, U. Müller, *The Journal of Neuroscience: The Official Journal of the Society for Neuroscience* 24 (2004) 3402–3412.
- [19] D.J. Solecki, X.L. Liu, T. Tomoda, Y. Fang, M.E. Hatten, *Neuron* 31 (2001) 557–568.
- [20] I. Rios, R. Alvarez-Rodriguez, E. Marti, S. Pons, *Development (Cambridge, England)* 131 (2004) 3159–3168.
- [21] R.S. Klein, J.B. Rubin, H.D. Gibson, E.N. DeHaan, X. Alvarez-Hernandez, R.A. Segal, A.D. Luster, *Development (Cambridge, England)* 128 (2001) 1971–1981.
- [22] D. Vaudry, B.J. Gonzalez, M. Basille, L. Yon, A. Fournier, H. Vaudry, *Pharmacological Reviews* 52 (2000) 269–324.
- [23] M. Basille, D. Cartier, D. Vaudry, I. Lihmann, A. Fournier, P. Freger, N. Gallo-Payet, H. Vaudry, B. Gonzalez, *The Journal of Comparative Neurology* 496 (2006) 468–478.
- [24] Y. Skoglösa, C. Patrone, D. Lindholm, *Neuroscience Letters* 265 (1999) 207–210.
- [25] H.S. Nielsen, J. Hannibal, J. Fahrenkrug, *Neuroreport* 9 (1998) 2639–2642.
- [26] A. Nicot, V. Lelièvre, J. Tam, J.A. Waschek, E. DiCicco-Bloom, *The Journal of Neuroscience: The Official Journal of the Society for Neuroscience* 22 (2002) 9244–9254.
- [27] V. Lelievre, A. Seksenyan, H. Nobuta, W.H. Yong, S. Chhith, P. Niewiadomski, J.R. Cohen, H. Dong, A. Flores, L.M. Liau, H.I. Kornblum, M.P. Scott, J.A. Waschek, *Developments in Biologicals* 313 (2008) 359–370.
- [28] T. Fila, S. Trazzi, C. Crochemore, R. Bartesaghi, E. Ciani, *The Journal of Biological Chemistry* 284 (2009) 15325–15338.
- [29] M.E. Hatten, W.-Q. Gao, M.E. Morrison, C.A. Mason, in: G. Bank, G. Kimberly (Eds.), *Cult. Nerve Cells*, The MIT Press, Cambridge, MA, 1998, pp. 419–460.
- [30] E.W. Humke, K.V. Dorn, L. Milenkovic, M.P. Scott, R. Rohatgi, *Genes & Development* 24 (2010) 670–682.
- [31] Y. Obara, A.M. Horgan, P.J.S. Stork, *Journal of Neurochemistry* 101 (2007) 470–482.
- [32] A.C. Emery, L.E. Eiden, *The FASEB Journal* 26 (2012) 3199–3211.
- [33] J. Ster, F. de Bock, F. Bertaso, K. Abitbol, H. Daniel, J. Bockaert, L. Fagni, *The Journal of Physiology* 587 (2009) 101–113.
- [34] P.J.R. Ocbina, K.V. Anderson, *Developmental Dynamics* 237 (2008) 2030–2038.
- [35] M. Barzi, J. Berenguer, A. Menendez, R. Alvarez-Rodriguez, S. Pons, *Journal of Cell Science* 123 (2010) 62–69.
- [36] H. Tukachinsky, L.V. Lopez, A. Salic, *The Journal of Cell Biology* 191 (2010) 415–428.
- [37] J. Kim, M. Kato, P.A. Beachy, *Proceedings of the National Academy of Sciences of the United States of America* 106 (2009) 21666–21671.
- [38] S.J. Beebe, P. Salomonsky, T. Jahnsen, Y. Li, *The Journal of Biological Chemistry* 267 (1992) 25505–25512.
- [39] L.V. Goodrich, L. Milenković, K.M. Higgins, M.P. Scott, *Science* 277 (1997) 1109–1113.
- [40] J.R. Cohen, D.Z. Resnick, P. Niewiadomski, H. Dong, L.M. Liau, J.A. Waschek, *BMC Cancer* 10 (2010) 676.